An Influence of Temperature on Additive Manufactured Composite with Embedded Fiber Bragg Grating Sensor

MAGDALENA MIELOSZYK, KATARZYNA MAJEWSKA, RUTA RIMASAUSKIENE, MARIUS RIMASAUSKAS and TOMAS KUNCIUS

ABSTRACT

Additive manufacturing (AM) is a name for techniques applied to constructing three-dimensional (3D) objects in a layer-by-layer process. AM methods can be applied for creating elements from fiber (glass/ carbon) reinforced polymers. During the process, fiber Bragg grating (FBG) sensors can be embedded into the element structure for the purpose of structural health monitoring (SHM) system development. Such an approach combines in one, advantages of AM (limited waste, elements with complex shape) and SHM system (safety, information about real loading conditions). Such a method can be applied for the manufacturing of different elements applied in many branches of industry, e.g. marine or civil engineering.

The goal of the paper is to analyze the temperature influence on AM fiber (glass/ carbon) reinforced polymer structures with embedded FBG sensors. The analyzes will be focused on the influence of FBG sensors on material durability. Additionally, the influence of elevated temperatures on the finished AM elements will be investigated.

INTRODUCTION

Additive manufacturing (AM) techniques are applied to constructing 3D objects in a layer-by-layer process from a variety of materials. Such methods allow manufacturing elements with complex shapes and limited amount of waste producing during the process. Some AM methods can be applied for producing structures from fiber reinforced polymers (FRP). As a reinforcement carbon [1] or glass [2] fibres can be used.

AM allows to embed optical sensors during the manufacturing process and apply them for measurement mechanical parameters of the structures [3, 4]. Optical sensors have many advantages (e.g. small size and low weight, high corrosion resistance, no electric field, low signal attenuation) that allow them to be embedded into FRPs. One of

Magdalena Mieloszyk, Email: mmieloszyk@imp.gda.pl. Institute of Fluid Flow Machinery, Polish Academy of Sciences, Fiszera 14, 80-231 Gdansk, Poland
Katarzyna Majewska, Institute of Fluid Flow Machinery, Polish Academy of Sciences, Fiszera 14, 80-231 Gdansk, Poland
Ruta Rimasauskiene, Marius Rimasauskas, Tomas Kuncius, Kaunas University of Technology, Studentu 56, 51424 Kaunas, Lithuania

the optical fibre sensors are fiber Bragg grating (FBG) sensors that embedded into the element structure or mounted on their surfaces can be applied for structural health monitoring (SHM). SHM systems based on FBG sensors can be applied in many branches of industry, e.g. marine [5] or civil engineering [6].

FRP have many advantages like: low weight, high resistance to environmental factors and fatigue loads [7]. Such features of FRP results in replacement of metal by them. Due to this FRP elements are exploited in a variety of environmental and loading conditions.

The aim of the paper is to compare the behaviour of AM carbon fiber reinforced polymer (CFRP) and glass fiber reinforced polymer (GFRP) samples with FBG sensors exposed to elevated temperatures.

The paper is organised as follows. Firstly, AM samples with FBG sensors and used AM method will be described. Then experimental results related to strain determined for different temperature values will be shown. Finally, some conclusions are drawn.

MANUFACTURING METHOD & SAMPLES

The analyses were performed on CFRP and GFRP samples manufactured using modified fused deposition modelling (FDM) method. The used components were as follow: polylactic acid (PLA) and continuous carbon fiber (T300B-3000) or continuous glass fiber (EC11 300). In order to improve printability of fibers material was impregnated before the printing process started. AM was performed using 3D printer (MeCreator 2). The details of the AM procedure (described for CFRP material) was presented in [8].The main printing parameters, used during the AM of the samples, are collected in Table I.

A photograph of FRP samples after manufacturing are presented in Figure 1. In the middle of each sample (between the second and the third layer) an FBG sensor was embedded during the AM process. The second FBG sensor was attached using cyanoacrylate glue to the sample surface. Both sensors had 10 mm gauge length and were located parallel to the main axis of the sample and the continuous fibers directions. The schema of a sample with marked locations of FBG sensors is presented in Figure 2. The dimensions of both sample types (CFRP and GFRP) are collected in Table II.

TABLE I. Chosen 3D printing parameters.

Printing settings	CFRP	GFRP
Nozzle (stainless steel) diameter [mm]	1.5	1.5
Extrusion multiplier	0.7	0.8
Extruder temperature [°C]	210	220
Build platform temperature [°C]	80	80
Printing speed [mm/min]	180	180
Line width [mm]	1.6	1.3
Layer height [mm]	0.5	0.5
Fiber orientation	Unidirectional 0°	Unidirectional 0°
Infill ratio [%]	100	100

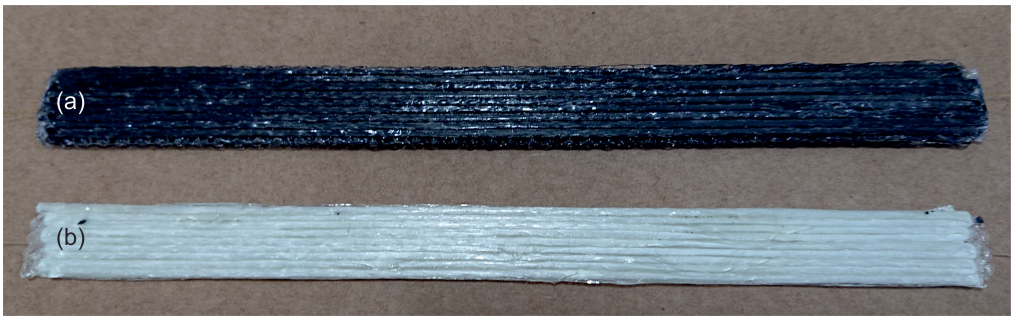

Figure 1. Photograph of analysed samples: (a) CFRP, (b) GFRP.

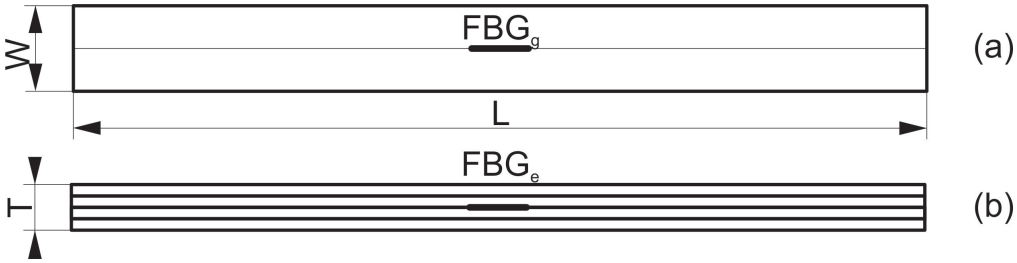

Figure 2. Schema of sample with FBG sensors locations on: (a) upper surface, (b) cross-section of the sample; FBG$_g$ – glued FBG sensor, FBG$_e$– embedded FBG sensor, W – width, L – length, T – thickness.

TABLE II. Sample dimensions.

	Sample			Layer	
Material	Length [mm]	Width [mm]	Thickness [mm]	Number	Stacking sequence
CFRP	150	15	2	4	[0,0]s
GFRP	150	12	2	4	[0,0]s

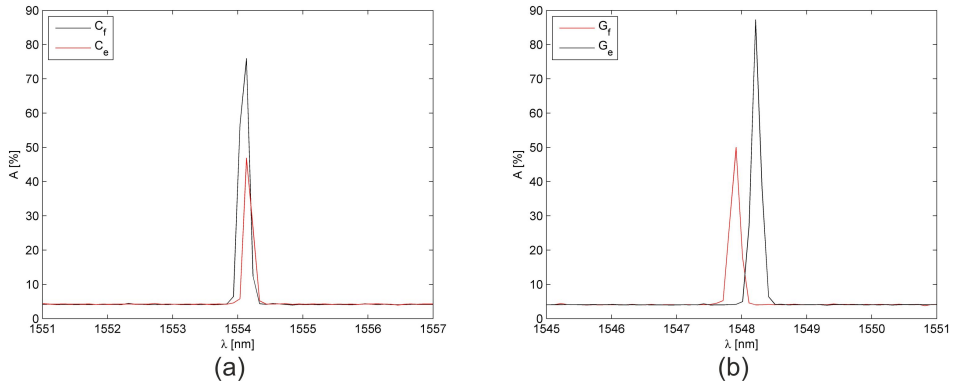

Figure 3. A comparison of FBG sensors spectra for (a) CFRP, (b) GFRP; f – free, e – embedded.

An example of comparison of FBG sensor spectra before and after embedding is presented in Figure 3. The embedding process caused reduction of the sensor reflectivity for both sample types. Regardless of the reflectivity value for free sensor, its value after embedding has the similar level – ca. 50%. There was no influence of the AM process on spectra shapes. In CFRP samples the residual strains related to the manufacturing process are neglected. While in GFRP sample a compression was observed resulted in strain value equal to 3.64x10^{-4} m/m.

EXPERIMENTAL INVESTIGATION

The measurements of the elevated temperature influence was performed in environmental chamber MyDiscovery DM600C (Angelantoni Test Technologies Srl, Italy). During the investigation, three samples of each type (GFRP and CFRP) were used. The samples were kept on a lattice shelf to allow them to expand in all directions. The measurements were performed using interrogator si425-500 from Micron Optics with a measurement frequency equal to 1 Hz.

The samples were exposed to nine temperature values from a range of 10°C to 50°C with a step of 5°C. The investigations were performed under stable relative humidity (RH) level equal to 20%.

Total strain values for all FBG sensors was calculated using the following equation:

$$\varepsilon_c(T) = \frac{\lambda_m(T) - \lambda_b(T)}{\lambda_b(T)} \tag{1}$$

where λ_m and λ_b are measured and base Bragg wavelengths, respectively. The base condition temperature was equal to 20°C. Total strain values contain both mechanical strain in FRP materials and temperature influence on FBG sensor and the fibre optic material.

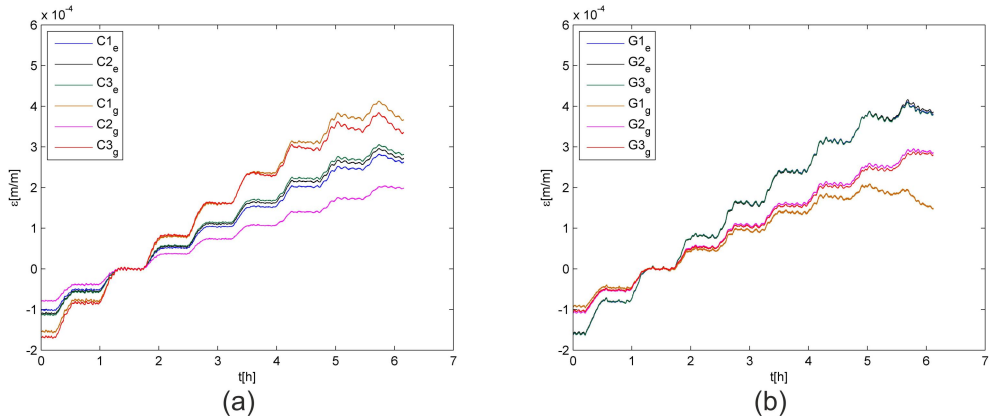

Figure 4. A comparison of total strain for (a) CFRP, (b) GFRP; C – CFRP, G – GFRP, f – free, e – embedded.

TABLE III. Strain differences among chosen FBG sensors; C – CFRP, G – GFRP .

Strain differences [mm/mm]	CFRP	GFRP
(Cx_g-Cx_e) $_{max}$ or (Gx_g-Gx_e) $_{max}$ for x=1,2,3	$8.2x10^{-5}$	$7.1x10^{-5}$
(Cx_g-Cy_g)$_{max}$ or (Gx_g-Gy_g)$_{max}$ for x=1,2,3 and y=1,2,3	$11.5x10^{-5}$	$8.4x10^{-5}$
($C1_e$+$C2_e$+$C3_e$)/3 or ($G1_e$+$G2_e$+$G3_e$)/3	$6x10^{-6}$	$2x10^{-6}$

A comparison of total strain curves determined for FBG sensors embedded or attached to the surfaces of CFRP and GFRP samples is presented in Figure 4. The characteristic shapes of the strain curves are related to the heating program in the chamber. It is worth mentioning, that the strain curves determined for FBG sensors embedded in the samples are similar for all sensors in each group (CFRP and GFRP). On contrary to this, the strain values determined from FBG sensors attached to the samples surfaces strongly depend on the exact location of each analysed sensor. Sensors were glued to the fibre bundles, polymeric matrix or to both materials. Due to the wider carbon fibre bundles it is possible to distinguish FBG sensors attached to fibres ($C3_g$) and matrix ($C1_g$ and $C2_g$). Strain values for $C3_g$ sensor are lower than for the embedded ones while for $C1_g$ and $C2_g$ are higher. For GFRP samples strain values for all attached sensors are smaller than for the embedded ones. The strain values were determined with the accuracy $3x10^{-6}$ [m/m], while the temperature with the accuracy of 0.32°C.

Then the mechanical strain in FRP material was determined using the following relationship:

$$\varepsilon_t(T) = \varepsilon_c(T) - \varepsilon_f(T) \tag{2}$$

where ε_f is strain determined experimentally for free FBG sensor exposed to temperature.

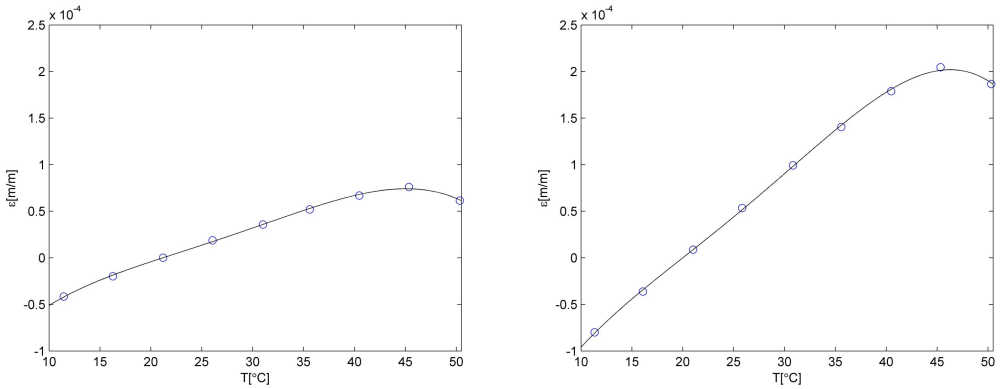

Figure 5. A comparison of thermal strain values for (a) CFRP, (b) GFRP; circles – measured values, continuous line – approximation.

TABLE IV. Comparison of strain values and coefficient of thermal expansion (CTE).

Parameters	CFRP	GFRP
Maximal strain (at 45°C)	7.6x10^{-5} [mm/mm]	20.1x10^{-5} [mm/mm]
Strain at 10°C	-5.1x10^{-5} [mm/mm]	-9.5x10^{-5} [mm/mm]
Strain at 50°C	6.3x10^{-5} [mm/mm]	18.2x10^{-5} [mm/mm]
CTE	3.74x10^{-6} [1/°C]	8.88x10^{-6} [1/°C]

A comparison of the strain differences among chosen FBG sensors is presented in Table III. It shows that the maximal differences among sensors in the same sample (embedded and attached) are comparable for both materials. The differences between CFRP and GFRP are equal to ca. 12%. The mean strain differences (for the same temperature) among the embedded sensors are close to the accuracy level of the interrogator (1x10^{-6}).

It allows to determine the relationship between strain in FRP materials and temperature. A comparison of strain values for both FRP materials determined for nine temperature values (measurement points) is presented in Figure 5. The presented strain values are the mean strain values from three FBG sensors embedded in each FRP material. For both materials the higher strain values are observed for 45°C. Then the strain decrease is observed. The similarity in both GFRP and CFRP samples suggests the behaviour of PLA matrix and its sensitivity on the temperature influence. The details of the observed phenomena for AM CFRP were described in [9].

A comparison of strain values for three chosen temperatures and coefficient of thermal expansion (CTE) for GRFP and CFRP are presented in Table IV. The CTE values were determined for a range of 10°C to 40°C. The achieved CTE values are similar to those for FRP materials presented in literature for samples manufactured using standard production methods. CTE for GFRP is in the range of 5.4x10^{-6} [1/°C] to 9.1x10^{-6} [1/°C] depends on the amount (weight quantity) of epoxy and hardener in the polymeric matrix [10]. While for CFRP the CTE values are in the range of 1.2x10^{-6} [1/°C] to 1.9x10^{-6} [1/°C] [11].

The achieved experimental CTE values for AM GFRP material is within the range given in the literature. While for the AM CFRP material CTE values are ca. 2 times higher than presented in [11]. However it is still in the acceptable level as due to high strength and high modulus of carbon fibers, the CTE of CFRP composites are generally below 10x10^{-6} [1/°C] [11].

CONCLUDING REMARKS

In the paper, two types of AM FRP samples (CFRP and GFRP) fabricated using the same manufacturing method were analysed. Inside every sample an FBG sensor was embedded, while the second sensor was attached to its surface. The main differences among the samples were related to the used reinforcement – glass or carbon continuous fibre.

The samples were exposed to elevated temperatures (from 10°C to 50°C). On FBG sensors mounted on the samples surfaces local character of the sensors was observed. The stain values were higher for sensors glued to PLA matrix than to fibre. It was espe-

cially visible for CFRP as carbon fibre bundles were wider and it was possible to attach the sensor to the fibres only. The strain values determined from embedded sensors were similar for all samples from the same group (CFRP or GFRP). The mean differences were not higher than $6x10^{-6}$ [m/m] while the accuracy level of the interrogator was $1x10^{-6}$ [m/m]

It allows to determine the relationships between strain and temperature and determine the CTE values for both materials. Due to the PLA matrix behaviour resulted in strain increasing up to 45°C and decreasing for higher temperatures, CTE values change with temperature. The CTE values were determined for the temperatures from the range of 10°C to 40°C, only.

ACKNOWLEDGMENT

This research was supported by the project entitled 'Additive manufactured composite smart structures with embedded fiber Bragg grating sensors (AMCSS)' funded by the National Science Centre, Poland under M-ERA.NET 2 Call 2019, grant agreement 2019/01/Y/ST8/00075.

The opinions expressed in this paper do not necessarily reflect those of the sponsors.

REFERENCES

1. Karaş, B., P. J. Smith, J. P. A. Fairclough, and K. Mumtaz. 2022. "Additive manufacturing of high density carbon fibre reinforced polymer composites," *Additive Manufacturing*, 58:103044.
2. Dickson, A. N., J. N. Barry, K. A. McDonnell, and D. P. Dowling. 2017. "Fabrication of continuous carbon, glass and Kevlar fibre reinforced polymer composites using additive manufacturing," *Additive Manufacturing*, 16:146–152.
3. Nagulapally, P., M. Shamsuddoha, T. Herath, L. Djukic, and G. B. Prusty. 2023. "Mechanical and optical performance evaluations of embedded polyimide and PEEK coated distributed optical sensors in glass fibre reinforced composites with vinyl ester resin systems," *Journal of Composite Materials*, 57(10):1707–1728.
4. Mieloszyk, M., K. Majewska, A. Andrearczyk, R. Rimasauskiene, M. Rimasauskas, and A. Orlowska. 2022. "The thermal influence on additive manufactured composite with fiber Bragg grating sensor," in *Proceedings of SPIE - The International Society for Optical Engineering*, vol. 12048.
5. Roberts, G. W., C. M. Hancock, W. Lienhart, F. Klug, N. Zuzek, and H. de Ligt. 2021. "Displacement and frequency response measurements of a ship using GPS and fibre optic-based sensors," *Applied Geomatics*, 13:51–61.
6. Feng, P., X. Meng, J.-F. Chen, and L. Ye. 2019. "Mechanical properties of structures 3D-printed with cementitious powders," in *3D Concrete Printing Technology*, Elsevier, pp. 181–209.
7. Tuwair, H., J. Volz, M. ElGawady, M. Mohamed, K. Chandrashekhara, and V. Birman. 2016. "Behavior of GFRP bridge deck panels infilled with polyurethane foam under various environmental exposure," in *Structures*, Elsevier, vol. 5, pp. 141–151.
8. Rimašauskas, M., T. Kuncius, and R. Rimašauskienė. 2019. "Processing of carbon fiber for 3D printed continuous composite structures," *Materials and Manufacturing Processes*, 34(13):1528–1536.

9. Muna, I. I. and M. Mieloszyk. 2021. “Temperature Influence on Additive Manufactured Carbon Fiber Reinforced Polymer Composites,” *Materials*, 14(21):6413.
10. Vaggar, G. B., S. Kamate, P. Badyankal, et al. 2018. “Thermal properties characterization of glass fiber hybrid polymer composite materials,” *Int. J. Eng. Technol*, 7:455–458.
11. Dong, C., K. Li, Y. Jiang, D. Arola, and D. Zhang. 2018. “Evaluation of thermal expansion coefficient of carbon fiber reinforced composites using electronic speckle interferometry,” *Optics express*, 26(1):531–543.